

Application of graphene from exfoliation in kitchen mixer allows mechanical reinforcement of PVA/graphene film

Zulhelmi Ismail¹ · Abu Hannifa Abdullah² · Anis Sakinah Zainal Abidin² · Kamal Yusoh²

Received: 2 May 2017 / Accepted: 20 June 2017 / Published online: 26 June 2017
© The Author(s) 2017. This article is an open access publication

Abstract Mechanical properties of polyvinyl alcohol (PVA) can be reinforced from the addition of graphene into its matrix. However, pristine graphene lacks solubility in water and thus makes dispersion a challenging task. Notably, functionalisation of graphene is required to accommodate graphene presence in the water. In this work, we have used a kitchen mixer to produce gum Arabic–graphene (G_{GA}) for the first time as filler for mechanical reinforcement of PVA. For the characterisation of exfoliated graphene, mean lateral size of G_{GA} was measured from the imaging by transmission electron microscopy while the mean thickness of graphene was predicted from the obtained spectra by Raman spectroscopy. During the preparation of PVA/graphene film by solution casting, G_{GA} was varied between 0, 0.05, 0.075, 0.10 and 0.15 wt% in concentration. We found that the presence of G_{GA} in PVA improves the tensile stress and elastic modulus about 72–200 and 19–187% from the original values. The data from Halpin–Tsai meanwhile suggested that the mechanical reinforcement of PVA/graphene film is due to the random distribution network of G_{GA} in PVA.

Keywords Graphene · Gum Arabic · Exfoliation · Kitchen mixer · Mechanical reinforcement · PVA/graphene

Introduction

Polyvinyl alcohol (PVA) is a synthetic polymer that is produced from the chemical conversion of polymerised vinyl acetate in a hydrous methanol (Cline et al. 1952). In addition to zero toxicity, the presence of high number of OH bonds in PVA is also allowing high solubility of PVA in water. Despite these advantages, the reported values of tensile strength, σ (15.7–74 MPa) for pristine PVA (Chen et al. 2005; Liang et al. 2009; Liu et al. 2005) are remarkably lower than that of industrial polymer such as nylon 6 (Cho and Paul 2001; Zhang et al. 2004). To improve the mechanical characteristic of PVA, reinforcement by filler is very important as the selected filler must not only enhance the tensile strength of PVA, but also have good interfacial interactions with PVA.

Due to the excellent mechanical properties of graphene, it is the most suitable candidate for mechanical improvement of PVA. However, pristine graphene is hydrophobic in nature and this makes the dispersion of graphene in a hydrophilic polymer like PVA unfeasible. To overcome this challenge, graphene oxide (GO) was commonly used as a filler for PVA due to high solubility of GO in water (Liang et al. 2009). The H-bonding between PVA and GO was suggested as a major mechanism in homogeneous distribution of GO in the matrix of PVA. Moreover, the pre-dispersion of GO in PVA would allow reduction of GO to graphene, as been demonstrated by the change from a brownish film of PVA to opaque black after the reduction stage of the PVA/GO film (Kashyap et al. 2016; Zhou et al. 2011). Currently, functionalisation of graphene with PVA has even been reported for better distribution of graphene in the matrix (Arao et al. 2016). In their work, sonication and pressure homogeniser were used in the exfoliation of graphite to graphene.

✉ Zulhelmi Ismail
zulhelmiismail.ump@gmail.com

¹ Faculty of Manufacturing Engineering, Universiti Malaysia Pahang, 26600 Pekan, Pahang, Malaysia

² Faculty of Chemical Engineering and Natural Resources, Universiti Malaysia Pahang, 26300 Kuantan, Pahang, Malaysia

While better mechanical performance was observed for PVA with the incorporation of PVA–graphene synthesised by pressure homogeniser, the application of kitchen mixer as a tool for preparation of gum Arabic–graphene (G_{GA}) in the mechanical reinforcement of PVA until now has never been discussed. A majority of works on PVA/graphene composite used sonication as a method for production of graphene (Al Islam et al. 2016; Jan et al. 2016). It is expected that the presence of biocompatible G_{GA} in the matrix would allow the future usage of PVA as material for biomedical and biological application. Therefore, it is important to show that the mechanical reinforcement of PVA can still be achieved from the incorporation of G_{GA} by a kitchen mixer as an exfoliating device.

Herein, we report the application of shear exfoliated G_{GA} as filler for the mechanical reinforcement of PVA. The graphene was prepared from the mixing of graphite and gum Arabic in a kitchen mixer of 800 W. We found that G_{GA} was easily dispersed in the solution of PVA and the resulting PVA/graphene film performed mechanically better than original PVA. In addition, the developed PVA/graphene film also has higher thermal stability than that of pure PVA.

Results and discussion

Characterisations of graphene

To establish that the graphene indeed was produced during the exfoliation in a kitchen mixer, the imaging of graphene in the supernatant was carried out by transmission electron microscopy (TEM). We washed the supernatant in multiple cycles to remove the presence of unbound gum Arabic on the G_{GA} sheets prior to the deposition on copper grid. Figure 1 shows the transparency level of deposited G_{GA} against grid background, which could be used to confirm the thin layer nature of graphene. The wrinkleless sheets

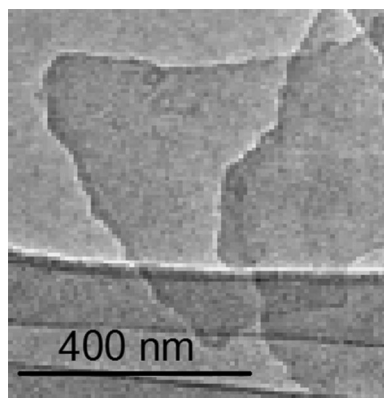


Fig. 1 TEM image of exfoliated graphene

here indicate the absence of defect on the graphene surface after functionalisation with gum Arabic (Chabot et al. 2013; Fan et al. 2012). Sharp edges of graphene sheets meanwhile were caused by fragmentation mechanism during the exfoliation stage (Paton et al. 2014). TEM statistical length distribution of G_{GA} shows that the mean lateral size, $\langle L \rangle$ of graphene after exfoliation is 450 nm. The value definitely is in range with the reported $\langle L \rangle$ exfoliated graphene by a mixer (Varrla et al. 2014) and by high-shear mixer (Paton et al. 2014).

While TEM can be applied to measure the length of graphene, Raman spectroscopy data are useful for defect and thickness characterisations of resulting G_{GA} . The obtained Raman spectra for graphite and G_{GA} are presented in Fig. 2. We found distinct changes to a spectrum of graphene after exfoliation of graphite by a kitchen mixer. There are shifts of D (1348 – 1339 cm^{-1}), G (1576 – 1566 cm^{-1}) and 2D (2710 – 2682 cm^{-1}) bands toward smaller Raman numbers, which are indicating the strong effect of exfoliation on the structure of bulky graphite (Paton et al. 2014). To determine the defect level in our produced G_{GA} , the intensity ratios of defect and graphite band (I_D/I_G) for graphite and graphene were computed. We note that the value of I_D/I_G for graphene only slightly increases to 0.11 as compared to that of graphite which is 0.032. This minor difference indicates that the exfoliation by a kitchen mixer did not introduce significant defect to the structure of produced G_{GA} in this work.

The mean layer number $\langle N \rangle$ of G_{GA} meanwhile was evaluated from the Raman data through intensity ratio measurement of full-width half maximum (FWHM) for 2D band (Green and Hersam 2009). Based on the resulting FWHM of 2D band for our graphene (86 cm^{-1}), and reported FWHM of 2D band for monolayer graphene (35 cm^{-1}) (Green and Hersam 2009), the produced value of $\langle N \rangle$ for G_{GA} seems to imply that majority of G_{GA} sheets are bilayer when only FWHM of 2D band was concerned.

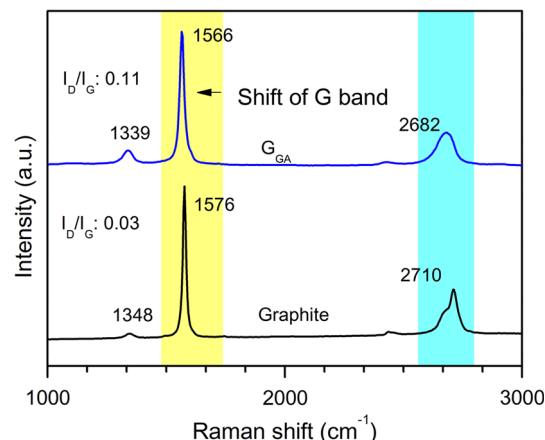


Fig. 2 Typical Raman spectra of graphite and G_{GA}

However, this resulting value is not accurate enough as the proposed metric is only suitable for thickness measurement of single graphene sheet (Green and Hersam 2009) and not for vacuum-filtered graphene film. Moreover, our produced graphene is not as pristine as the metric required due to its functionalisation with gum Arabic. Therefore, we have to use another metric for estimation of $\langle N_G \rangle$ of our graphene (Backes et al. 2016):

$$\langle N_G \rangle = 0.83e^{3.6M} \quad (1)$$

$$M = \frac{I_{\text{Graphene at } \omega = \omega_{\text{Peak of Graphite}}}}{I_{\text{Graphite at } \omega = \omega_{\text{Peak of Graphite}}}} \bigg/ \frac{I_{\text{Graphene at } \omega = \omega_{\text{shoulder}}}}{I_{\text{Graphite at } \omega = \omega_{\text{shoulder}}}} \quad (2)$$

The published metric is suitable for the prediction of $\langle N_G \rangle$ from Raman study of vacuum-filtered graphene film and in addition is neglecting the effect of doping or functionalisation on graphene sheet thickness (Backes et al. 2016). Assuming that the difference between the shoulder and peak of 2D band is -30 cm^{-1} (Paton et al. 2014), the value of M was computed as 0.51 and would result in the $\langle N_G \rangle$ value of $5.1 \sim 5$ layers with 18% deviation. This new result, however, is consistent with the 2D band pattern of our graphene, which is strikingly similar to the reported 2D band pattern of few-layer graphene previously (Ghoneim et al. 2013; Kim et al. 2012).

Characterisation of PVA/graphene

Chemical interaction

To investigate the change of PVA composition after the presence of G_{GA} , we carried out spectra measurements of PVA and PVA/graphene film using infrared spectroscopy (IR). For confirmation of graphene dispersion in the matrix of PVA, IR spectrum of G_{GA} was also collected. The

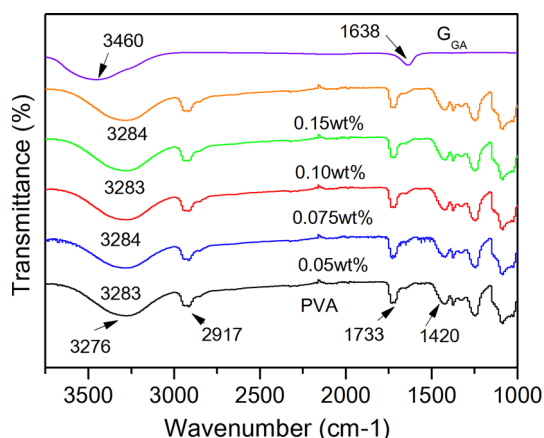


Fig. 3 FTIR spectra for G_{GA} , PVA and PVA/graphene with 0.05, 0.075, 0.10 and 0.15 wt% concentrations

resulting spectra for G_{GA} , PVA and PVA/graphene film are presented in Fig. 3.

It is clear that the difference between the spectra of PVA and PVA/graphene films is very minor. We note that there is a shift of IR band at 3276 cm^{-1} towards higher wavenumber ($3283\text{--}3284 \text{ cm}^{-1}$), which indicates the increase of H-bonds in PVA after G_{GA} addition. In addition, this shift is independent of graphene content as the shift rate is fixed at 6 or 7 cm^{-1} for all PVA/graphene samples. Based on this observation, we propose that the interaction between PVA and G_{GA} can only be achieved at certain concentration threshold of graphene ($<0.05 \text{ wt\%}$). We also notice that the increase of H-bonds in the macromolecular structure of PVA is in contrast to the previous reported finding on the PVA/graphene film (Yang et al. 2010). It is important to point out the effect of preparation for resulting IR spectra in this work. While reduction of graphene oxide to graphene was responsible for the dissociation of H-bonds in the structure, the increase of H-bonds in our PVA may be caused by the direct dispersion of G_{GA} in the matrix. The presence of oxygen groups on G_{GA} (Chabot et al. 2013; Fan et al. 2012) has led to the increase of more oxygen content in PVA. The evidences for a complete dispersion of graphene in PVA are provided by the shift of IR band at 3460 cm^{-1} and elimination of IR peak at 1638 cm^{-1} in the spectra of PVA/graphene films.

Thermal stability

To test the effect of graphene presence in PVA against heat, we conducted thermogravimetric analysis (TGA) and differential gravimetric analysis (DTG) testing on PVA and PVA/graphene film with 0.05 and 0.15 wt% concentrations. We found a minor shift of typical TGA curves for PVA/graphene films towards higher temperature, which is indicating a change of thermal resistivity for PVA after G_{GA} incorporation. This observation is consistent with the previous reported effect of graphene on the thermal properties of PVA (Guo et al. 2011; Liang et al. 2009). From the presented DTG curves of the same samples, we identify the onset temperature, T_{on} shift to 345 from $335 \text{ }^{\circ}\text{C}$ for PVA/graphene film with 0.05 wt% concentration. However, the shift of T_{on} is only $+5 \text{ }^{\circ}\text{C}$ when higher graphene contents were incorporated into PVA. We assume that the thermal stability of PVA is very sensitive to the presence of agglomerated G_{GA} sheets as higher addition of graphene tends to stack together in the matrix. In terms of the decomposition phase, the presence of G_{GA} in PVA did not induce any change towards the decomposition route of PVA (Yang et al. 2010). The resultant TGA and DTG curves of discussed samples are shown in Fig. 4.

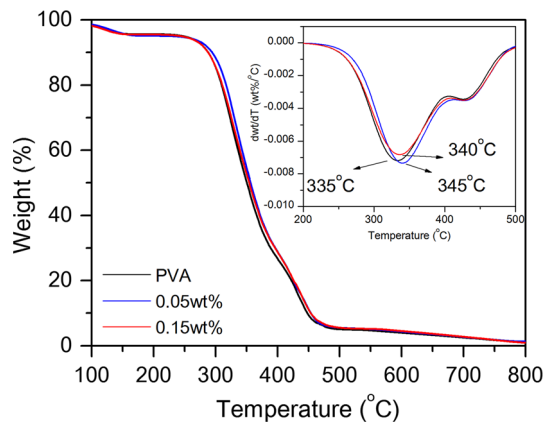


Fig. 4 Typical TGA and DTG curves for PVA and PVA/graphene film with 0.05 and 0.15 wt% concentrations

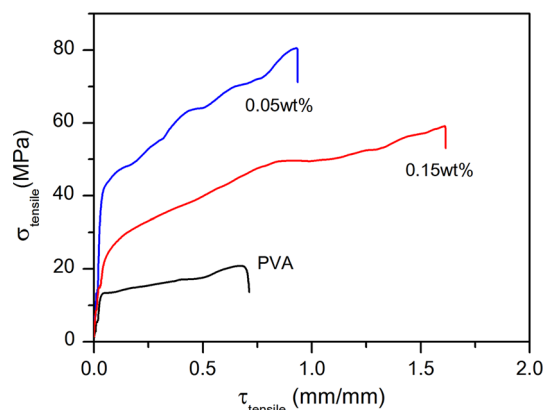


Fig. 5 Tensile plots for PVA and PVA/graphene films at 0.05 and 0.15 wt% concentrations

Mechanical properties

We used tensile plots (Fig. 5) and normalised tensile data (Fig. 6) for PVA and PVA/graphene films to highlight the mechanical reinforcement of PVA after the addition of graphene. Impressively, the presence of G_{GA} in PVA is observed to increase the tensile stress, σ about 72–200% and Young's modulus, E about 19–187% from the original value of PVA. Importantly, the increase of σ and E was applied for all PVA/graphene films without interference from incorporated G_{GA} contents in the matrix. However, the effect of agglomerated graphene in PVA was clear from the reduction of σ and E for samples with G_{GA} mass higher than 0.05 wt% concentration. As indicated previously, the even dispersion of G_{GA} in solution casted film of PVA could only be achieved at certain concentration levels of graphene. Aside from dispersion quality of G_{GA} , it is suggested that the tremendous improvement in σ and E for PVA with 0.05 and 0.15 wt% of G_{GA} was caused by the length distribution of graphene produced in this work. As reported previously (May et al. 2012), the aspect ratio of

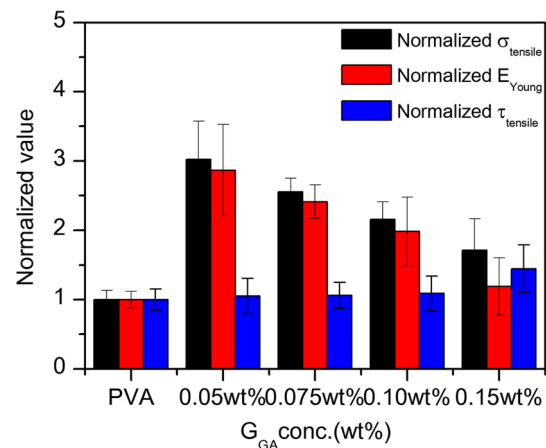


Fig. 6 Normalised tensile data for PVA and PVA/graphene films

graphene indeed can influence the σ and E values. For mechanical reinforcement of composite, load distribution between filler and matrix is preferable for filler with large dimensional area.

We also notice the increase in elongation rate of PVA after G_{GA} addition in matrix. As suggested by theory, the presence of stacked graphene structure from agglomeration acted as a sliding point, which allowed the increase of strain at higher graphene content (Zhao et al. 2010). With this in mind, we observed the increase in σ for PVA/graphene film at maximum for samples with 0.05 wt% concentration albeit the presence of sheets agglomeration. At higher G_{GA} contents, the dropped value of σ was due to the possible presence of more agglomeration regions in the matrix. This observation shows the limitation in our proposed method for preparation of PVA/graphene film. The resulting graphene from exfoliation by a kitchen mixer tends to cause restacking at higher G_{GA} contents during solution casting due to the large surface area possessed by a single graphene sheet. Hence, only low concentrations of G_{GA} are permitted to achieve even dispersion of graphene in the PVA matrix. In spite of the presented issue, the presence of H-bonding between PVA and G_{GA} was validated from the tensile strength reinforcement of the PVA with 0.05 and 0.15 wt% of graphene.

Previously, we used IR to investigate the chemical interaction between G_{GA} and PVA for PVA/graphene film. The interfacial interaction between both materials allows the improvement in mechanical properties of PVA/graphene films as compared to that of unmodified PVA. However, it was proposed that the aspect ratio and orientation of filler can also affect the Young modulus of PVA aside the interfacial interactions factor (Liang et al. 2009; May et al. 2012). As suggested by the well established Halpin–Tsai model, a modulus of composite can be dictated from the parallel distributed or randomly dispersed filler in the host polymer network (Affdl and Kardos 1976).

It is apparent that the orientation of G_{GA} in PVA matrix must be studied to evaluate the actual distribution pattern that has led to the increase of E value for PVA film in this work. Herein, we investigate the possible distribution of G_{GA} in PVA from a comparison study between predicted E values against experimentally determined results of E . In a parallel and randomly distributed graphene system, the value of E is expressed as (Affdl and Kardos 1976):

$$E_{\text{par}} = E_{\text{PVA}} \left(\frac{1 + \eta_L \varepsilon V_G}{1 - \eta_L V_G} \right) \quad (3)$$

$$E_{\text{rand}} = E_{\text{PVA}} \left[\frac{3}{8} \left(\frac{1 + \varepsilon \eta_L V_G}{1 - \eta_L V_G} \right) + \frac{5}{8} \left(\frac{1 + 2\eta_T V_G}{1 - \eta_T V_G} \right) \right] \quad (4)$$

with,

$$\eta_L = \frac{(E_G/E_{\text{PVA}}) - 1}{(E_G/E_{\text{PVA}}) + \varepsilon} \quad (5)$$

$$\eta_T = \frac{(E_G/E_{\text{PVA}}) - 1}{(E_G/E_{\text{PVA}}) + 2} \quad (6)$$

and,

$$\varepsilon = \frac{2L}{3t} \quad (7)$$

where E_{PVA} and E_G are the elastic modulus for PVA (400 MPa) and graphene. In this work, the value of E_G was taken as 0.25 TPa (Gómez-Navarro et al. 2008). The symbols of η_L and η_T are known as longitudinal and transverse constant while ε is the aspect ratio of used filler, which in this case is G_{GA} . We substituted the values of L and t in Eq. 5 with pre-determined values of 450 and 1.75 nm (5 layers) from TEM and Raman spectroscopy. The volume fraction of G_{GA} , V_G meanwhile was computed through the multiplication wt% with ρ_{PVA}/ρ_G . In this work, the PVA density, ρ_{PVA} is considered as 1.3 g cm⁻³ while the density value of G_{GA} , ρ_G was extracted from the density of graphite (2.2 g cm⁻³). The resultant plots of E , E_{par} and E_{rand} as function of V_G is presented in Fig. 7.

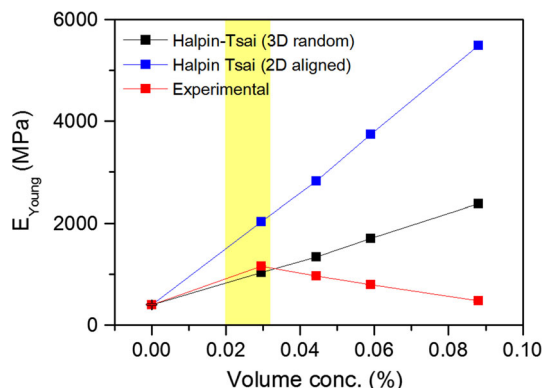


Fig. 7 Plotted line for E , E_{par} and E_{rand} estimates that majority of dispersed G_{GA} sheets in PVA are randomly distributed at 0.03 vol%

Surprisingly, we note that the resulting plot for experimental E intercepted the plot of E_{rand} , before dropping further below the line. This suggests that the increase of E for PVA/graphene is majorly contributed by randomly distributed graphene as higher content of G_{GA} would lead to the reduction of E value beyond the domain by agglomerated graphene sheets. This observation is against the previously reported reinforcement effect of graphene for PVA, which implies that the preferable orientation of graphene in matrix is parallel for efficient load distribution in the matrix (Liang et al. 2009; Yang et al. 2010). However, we also note that the elastic modulus reinforcement of PVA by graphene sheets could still be achieved by randomly distributed graphene sheets in the matrix (Zhao et al. 2010).

Physical and morphology

To confirm that the dispersion of G_{GA} indeed was possible in PVA, we photographed the resulting PVA and PVA/graphene films for the appearance study (see Fig. 8). It is clear that the change of PVA colour, which originally was colourless, to darker black at highest concentration of G_{GA} confirmed the possible dispersion of graphene from the exfoliation by a kitchen mixer albeit at the risk of agglomeration for PVA with higher content of graphene.

While visual observation is useful for the initial screening of G_{GA} dispersion state in PVA, we notice that a morphology study must be carried out to correlate the elongation increase from the previous mechanical study with the surface properties of PVA/graphene composite. To achieve this objective, we conducted multiple imaging of the fractured surface of PVA and PVA/graphene film by field emission scanning electron microscopy (FESEM). The resultant FESEM micrographs for PVA and PVA/graphene films with 0.15 wt% of G_{GA} are presented in Fig. 9. We observe the increase of ductility regions, which are represented by the wrinkled lines on the surface of PVA after the addition of graphene (Jose et al. 2015). These ductility regions are randomly distributed on the fractured surface while the ductility regions in pure PVA are

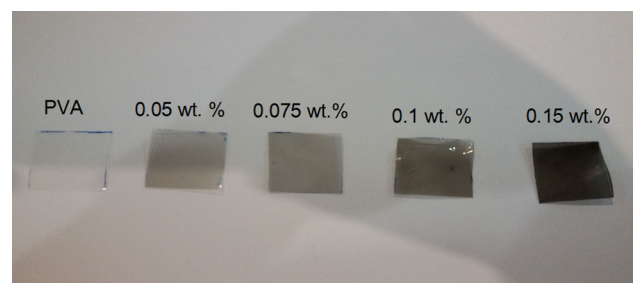


Fig. 8 Resulting PVA and PVA/graphene films with various concentrations of G_{GA}

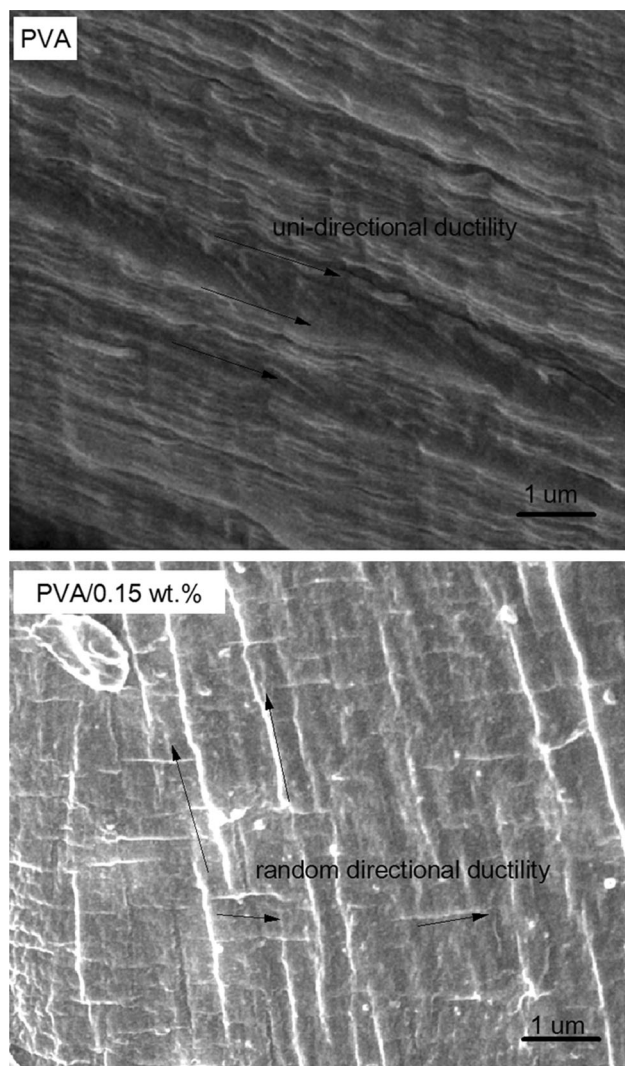


Fig. 9 FESEM fractured surface for PVA and PVA/graphene film with 0.15 wt% concentration of G_{GA}

pointing only unidirectionally. This observation for PVA/graphene composite may suggest the effect of randomly distributed G_{GA} in the matrix at higher graphene content as ductility of PVA/graphene film is mainly caused by the presence of stacking graphene in the matrix during the preparation stage (Zhao et al. 2010).

Conclusion

In this work, we have demonstrated the applicability of shear exfoliated graphene by a kitchen mixer for the mechanical reinforcement of PVA. In our exfoliation method, the prepared graphene was modified with gum Arabic to allow dispersibility of the material in water and stronger interfacial interactions with PVA. By comparing the tensile test data for PVA and PVA/graphene films, we

highlight the increase of σ and E after G_{GA} incorporation in PVA. It is also noticed from the Halpin–Tsai plot of modulus that the reinforcement effect in PVA/graphene is contributed by the random distribution of G_{GA} and not by parallel aligned G_{GA} sheets. However, we note that although the dispersion of G_{GA} was possible in PVA, the risk of sheets restacking at higher G_{GA} content ultimately limits the potential of casting as a preparation method for PVA/graphene film. Thus, a new dispersion approach for G_{GA} must be developed in the future to accommodate more graphene presence in PVA during casting. In spite of this presented issue, our proposed exfoliation route is considered a facile and green approach in the synthesis of gum Arabic-graphene. Using a kitchen mixer and gum Arabic, the prepared G_{GA} can be incorporated into PVA for mechanical reinforcement effect. This is likely to reduce the preparation cost of graphene and leading to progress in rapid prototyping of PVA/graphene composites.

Methods

Materials

Graphite (332461), gum Arabic (G9752) and PVA (341584) were purchased from Sigma Aldrich (Malaysia) and were used as received. Ultrapure water (Millipore) was utilised as dispersion medium for gum Arabic and PVA.

Preparation of graphene

In the preparation of gum Arabic–graphene (G_{GA}), we used a kitchen mixer (Philips, HR2096) to disperse 5 mg ml^{-1} of graphite sheet into 400 ml volume of gum Arabic/water. For optimum production of graphene, the exfoliation medium was prepared prior to the mixing by stirring 5 mg ml^{-1} of gum Arabic at 30°C . Total operation hour was set for 1 h with speed setting of 16 k rpm. The kitchen mixer was regularly stopped after mixing interval of 10 min due to the temperature increase of processed solution. We note that this is the technical weakness of kitchen mixer as the used motor was rapidly heated up after 10 min of operation. To avoid heat effect on the surface energy of the solution, water bath was used to cool the prepared graphene/graphite solution. After mixing, we used centrifugation at 3000 rpm for separation of G_{GA} from the unexfoliated graphite. The obtained supernatant then was washed through filtration of multiple stages before freeze drying.

Casting of PVA/graphene film

First we dissolved 1.5 g of PVA powder in 30 ml of water at the temperature of 80°C for 60 min. Then, the resulting

solution of PVA was left at ambient temperature for cooling for 30 min. In between, we carried out the dispersion of dried G_{GA} into PVA using bath sonication (Branson) with low power setting. The purpose was to avoid the introduction of defects on the graphene sheets as well as to protect PVA against molecular degradation by sonication. From the conducted weight measurement of dried G_{GA} prior to the redispersion, the solutions of PVA/graphene were prepared at different concentration percentage (0, 0.05, 0.075, 0.1 and 0.15 wt%) with total stirring duration of 24 h on the hot plate. The solution was then transferred into a Petri dish and left for drying in a hot oven at 60 °C overnight. The crystallised PVA/graphene film was then peeled from the Petri Dish and stored in desiccators equipped with silicate gels prior to the characterisation work.

Characterisation and equipment

Graphene

For the preparation of TEM imaging, we drop casted 0.5 ml of volume from the supernatant onto copper carbon grids (Cat.FF300- Cu) with 300 square meshes. To generate statistical distribution size of exfoliated G_{GA} , we measured the length of 100 graphene sheets using TEM Technai G2-20S-Twin (FEI). In the Raman spectroscopy characterisation, we used a vacuum-filtered graphene film as a sample. The graphene film was washed extensively prior to analysis to prevent the influence of excessive dispersant on D band graphene. We conducted Raman measurements on the graphene sample using WITec Alpha 300R model with excitation wavelength of 532.139 nm.

PVA/graphene film

Fractured surface of PVA strips from mechanical tensile test were studied using FESEM. Each of the sample surfaces were coated with platinum for production of clearer micrographs during the imaging by JEOL JSM 7800F. In the measurement of IR for PVA and PVA/graphene film, the IR analyses of samples were carried out on the previously casted film. To study the thermal stability of PVA after the presence of G_{GA} , we conducted thermal gravimetric analysis (TGA) on the samples using Mettler Toledo TGADSC1. Temperature of furnace was set between 25 and 900 °C with heating ramp of 10 °C min⁻¹. To avoid oxidation during the heating of the sample, nitrogen was purged in at the rate flow of 20 ml min⁻¹.

Prior to the tensile test measurement, 5 strips with dimension of 50 × 25 × 0.15 each were cut out from the casted film of PVA/graphene composite. Care was taken

during cutting of the strips as any presence of notches along the rectangular film boundary can affect the tensile measurements. These films were conditioned for 24 h prior to the testing in desiccators for removal of moisture from the film. During the testing, the strip was mounted between a pneumatic-powered clasper. A universal testing machine (Instron) with load cell of 250 N was employed for the measurement of the strips at the extension rate of 5 mm min⁻¹. The ambient temperature during the measurement was recorded at 26 °C.

Acknowledgements We acknowledge the Ministry of Higher Education of Malaysia and Universiti Malaysia Pahang for financial support (RDU 160149) throughout this research work. In addition, we are thankful to Science Engineering Research Centre (SERC) of Universiti Sains Malaysia and Institute of Advanced Technology (ITMA) of Universiti Putra Malaysia for providing technical assistance during TEM and Raman spectroscopy characterisation of graphene.

Open Access This article is distributed under the terms of the Creative Commons Attribution 4.0 International License (<http://creativecommons.org/licenses/by/4.0/>), which permits unrestricted use, distribution, and reproduction in any medium, provided you give appropriate credit to the original author(s) and the source, provide a link to the Creative Commons license, and indicate if changes were made.

References

- Affdl J, Kardos J (1976) The Halpin-Tsai equations: a review. *Polym Eng Sci* 16:344–352
- Al Islam MA, Rahman AM, Iftekhhar S, Salem KS, Sultana N, Bari ML (2016) Morphology, thermal stability, electrical, and mechanical properties of graphene incorporated poly(vinyl alcohol)-gelatin nanocomposites
- Arao Y, Mizuno Y, Araki K, Kubouchi M (2016) Mass production of high-aspect-ratio few-layer-graphene by high-speed laminar flow. *Carbon* 102:330–338
- Backes C et al (2016) Spectroscopic metrics allow in situ measurement of mean size and thickness of liquid-exfoliated few-layer graphene nanosheets. *Nanoscale* 8:4311–4323
- Chabot V, Kim B, Sloper B, Tzoganakis C, Yu A (2013) High yield production and purification of few layer graphene by gum Arabic assisted physical sonication. *Sci Rep* 3:1378
- Chen W, Tao X, Xue P, Cheng X (2005) Enhanced mechanical properties and morphological characterizations of poly(vinyl alcohol)-carbon nanotube composite films. *Appl Surf Sci* 252:1404–1409
- Cho J, Paul D (2001) Nylon 6 nanocomposites by melt compounding. *Polymer* 42:1083–1094
- Cline ET, Pinkney PS, Plambeck JL, Stevenson HB (1952) Water-resistant polyvinyl alcohol filament and process for producing same. Google Patents
- Fan J, Shi Z, Ge Y, Wang J, Wang Y, Yin J (2012) Gum arabic assisted exfoliation and fabrication of Ag-graphene-based hybrids. *J Mater Chem* 22:13764–13772
- Ghoneim MT, Smith CE, Hussain MM (2013) Simplistic graphene transfer process and its impact on contact resistance. *Appl Phys Lett* 102:183115

- Gómez-Navarro C, Burghard M, Kern K (2008) Elastic properties of chemically derived single graphene sheets. *Nano Lett* 8:2045–2049
- Green AA, Hersam MC (2009) Solution phase production of graphene with controlled thickness via density differentiation. *Nano Lett* 9:4031–4036
- Guo J, Ren L, Wang R, Zhang C, Yang Y, Liu T (2011) Water dispersible graphene noncovalently functionalized with tryptophan and its poly(vinyl alcohol) nanocomposite. *Compos B Eng* 42:2130–2135
- Jan R, Habib A, Akram MA, Khan AN (2016) Uniaxial drawing of graphene-PVA nanocomposites: improvement in mechanical characteristics via strain-induced exfoliation of graphene. *Nanoscale Res Lett* 11:377
- Jose J, Al-Harhi MA, AlMa'adeed MAA, Bhadra Dakua J, De SK (2015) Effect of graphene loading on thermomechanical properties of poly(vinyl alcohol)/starch blend. *J Appl Polym Sci* 132:149–168
- Kashyap S, Pratihari SK, Behera SK (2016) Strong and ductile graphene oxide reinforced PVA nanocomposites. *J Alloy Compd* 684:254–260. doi:[10.1016/j.jallcom.2016.05.162](https://doi.org/10.1016/j.jallcom.2016.05.162)
- Kim D, Han JY, Lee D, Lee Y, Jeon DY (2012) Facile conversion of a cellulose acetate laminate film to graphene by a lamination process and post-annealing. *J Mater Chem* 22:20026–20031
- Liang J, Huang Y, Zhang L, Wang Y, Ma Y, Guo T, Chen Y (2009) Molecular-level dispersion of graphene into poly(vinyl alcohol) and effective reinforcement of their nanocomposites. *Adv Func Mater* 19:2297–2302
- Liu L, Barber AH, Nuriel S, Wagner HD (2005) Mechanical properties of functionalized single-walled carbon-nanotube/poly(vinyl alcohol) nanocomposites. *Adv Func Mater* 15:975–980
- May P, Khan U, O'Neill A, Coleman JN (2012) Approaching the theoretical limit for reinforcing polymers with graphene. *J Mater Chem* 22:1278–1282
- Paton KR et al (2014) Scalable production of large quantities of defect-free few-layer graphene by shear exfoliation in liquids. *Nat Mater* 13:624–630
- Varrla E, Paton KR, Backes C, Harvey A, Smith RJ, McCauley J, Coleman JN (2014) Turbulence-assisted shear exfoliation of graphene using household detergent and a kitchen blender. *Nanoscale* 6:11810–11819
- Yang X, Li L, Shang S, X-m Tao (2010) Synthesis and characterization of layer-aligned poly(vinyl alcohol)/graphene nanocomposites. *Polymer* 51:3431–3435
- Zhang WD, Shen L, Phang IY, Liu T (2004) Carbon nanotubes reinforced nylon-6 composite prepared by simple melt-compounding. *Macromolecules* 37:256–259
- Zhao X, Zhang Q, Chen D, Lu P (2010) Enhanced mechanical properties of graphene-based poly(vinyl alcohol) composites. *Macromolecules* 43:2357–2363. doi:[10.1021/ma902862u](https://doi.org/10.1021/ma902862u)
- Zhou T, Chen F, Tang C, Bai H, Zhang Q, Deng H, Fu Q (2011) The preparation of high performance and conductive poly(vinyl alcohol)/graphene nanocomposite via reducing graphite oxide with sodium hydrosulfite. *Compos Sci Technol* 71:1266–1270